Arthritogenic alphaviral infection perturbs osteoblast function and triggers pathologic bone loss

Weiqiang Chen[a], Suan-Sin Foo[a], Nestor E. Rulli[a], Adam Taylor[a], Kuo-Ching Sheng[a], Lara J. Herrero[a], Belinda L. Herring[a], Brett A. Lidbury[b,1], Rachel W. Li[c], Nicole C. Walsh[d,e], Natalie A. Sims[d,e], Paul N. Smith[f], and Suresh Mahalingam[a,2]

[a]Emerging Viruses and Inflammation Research Group, Institute for Glycomics, Griffith University, Gold Coast, QLD 4222, Australia; [b]Department of Microbiology and Immunology, University of North Carolina at Chapel Hill, Chapel Hill, NC 27599-7290; [c]Trauma and Orthopaedic Research Laboratory, Department of Surgery, The Medical School, The Australian National University, John Curtin School of Medical Research, Canberra, ACT 2601, Australia; [d]St. Vincent's Institute, Fitzroy VIC 3065, Australia; [e]Department of Medicine at St. Vincent's Hospital, The University of Melbourne, Fitzroy VIC 3065, Australia; and [f]Trauma and Orthopaedic Research Unit, Department of Orthopaedic Surgery, The Canberra Hospital, Canberra, ACT 2605, Australia

Edited by Diane E. Griffin, Johns Hopkins Bloomberg School of Public Health, Baltimore, MD, and approved February 25, 2014 (received for review October 7, 2013)

Arthritogenic alphaviruses including Ross River virus (RRV), Sindbis virus, and chikungunya virus cause worldwide outbreaks of musculoskeletal disease. The ability of alphaviruses to induce bone pathologies remains poorly defined. Here we show that primary human osteoblasts (hOBs) can be productively infected by RRV. RRV-infected hOBs produced high levels of inflammatory cytokine including IL-6. The RANKL/OPG ratio was disrupted in the synovial fluid of RRV patients, and this was accompanied by an increase in serum Tartrate-resistant acid phosphatase 5b (TRAP5b) levels. Infection of bone cells with RRV was validated using an established RRV murine model. In wild-type mice, infectious virus was detected in the femur, tibia, patella, and foot, together with reduced bone volume in the tibial epiphysis and vertebrae detected by microcomputed tomographic (μCT) analysis. The RANKL/OPG ratio was also disrupted in mice infected with RRV; both this effect and the bone loss were blocked by treatment with an IL-6 neutralizing antibody. Collectively, these findings provide previously unidentified evidence that alphavirus infection induces bone loss and that OBs are capable of producing proinflammatory mediators during alphavirus-induced arthralgia. The perturbed RANKL/OPG ratio in RRV-infected OBs may therefore contribute to bone loss in alphavirus infection.

Interleukin-6 | Ross River virus disease | viral arthritis | osteoclastogenesis

Arthritogenic alphaviruses including Ross River virus (RRV), chikungunya virus (CHIKV), Sindbis virus (SINV), o'nyong-nyong virus (ONNV), and Barmah Forest virus (BFV) are classified under the genus *Alphavirus* ("Old World" alphaviruses) of the *Togaviridae* family (1). RRV is a small, enveloped, positive-sense single-stranded RNA virus transmitted by mosquitoes (2, 3). RRV disease (RRVD) in humans commonly affects the ankles, knees, and peripheral joints. The hallmarks of RRVD include incapacitating joint pain and polyarthralgias, with a level of disability comparable to rheumatoid arthritis (RA) (4, 5). Similar to RA, the onset of RRVD can be sudden and debilitating, and the prolonged manifestations of RRVD in some patients have been proposed to be due to the actions of proinflammatory mediators including interleukin-6 (IL-6), interleukin-1 (IL-1), and chemokine (C-C motif) ligand 2; monocyte chemotactic protein-1 (CCL2; MCP-1) (6–8).

Recently, bone lesions in joints of CHIKV-infected patients have been reported (9), providing evidence that alphavirus-induced disease can result in bone pathologies (10, 11). In physiological conditions, osteoblasts (OBs) form bone, and this cell lineage also expresses both receptor activator of nuclear factor-kappaB ligand (RANKL) and its soluble decoy receptor, osteoprotegerin (OPG). The expression of RANKL by the OB lineage is stimulated by IL-6 and IL-1β among other proinflammatory cytokines (12, 13), whereas CCL2 is thought to be an important chemoattractant for monocytic precursors during inflammatory processes (14, 15). Together with an elevation in RANKL/OPG ratio, this favors osteoclast (OC) formation from monocytic precursors (16, 17), leading to an increase in bone resorption and bone pathologies (18, 19). Despite the vital role OBs play in bone remodelling, their role in arthritogenic alphaviral infection and their potential contributions to alphaviral disease are not yet known.

In this study, we investigate the susceptibility and response of primary human OBs (hOBs) to RRV and the impact of RRV infection on bone. RRV infection of hOBs resulted in increased IL-6, IL-1β, and CCL2 together with an elevated RANKL/OPG ratio. Using microcomputed tomography (μCT), we report that alphavirus infection results in bone loss in an established RRV murine model. Collectively, these findings reveal that RRV can infect OBs and disrupt bone homeostasis, which may play an important role in alphavirus-induced arthritis by regulating proinflammatory cytokine/chemokine responses and pinpoint the significance of IL-6 in modulating bone loss by disrupting the balance of RANKL/OPG expression.

Results

RRV Replicates in Primary hOBs, Disrupts the RANKL/OPG Balance, and Induces Production of Proinflammatory Cytokines. To investigate OBs as a site of RRV replication, we assessed the ability of cultured hOBs to support RRV replication. The cultured hOBs were

Significance

Persistent polyarthritis, which occurs in 30–40% of alphavirus-infected patients, has been proposed to be caused by proinflammatory mediators such as IL-6. In the present study we investigated the susceptibility and response of primary human osteoblasts to Ross River virus (RRV) infection and determined whether infection could result in bone pathology. RRV infection of osteoblasts resulted in increased receptor activator of nuclear factor-kappaB ligand (RANKL) but decreased osteoprotegerin (OPG). We are the first to report that alphavirus infection results in bone loss in an established RRV murine model and that this bone loss is prevented by IL-6 inhibition. These findings reveal that RRV can disrupt bone homeostasis and that osteoblasts play an important role in alphavirus-induced arthritis by regulating IL-6 and contribute to bone loss by disrupting the RANKL/OPG balance.

Author contributions: W.C. and S.M. designed research; W.C., S.-S.F., N.E.R., A.T., and B.A.L. performed research; S.-S.F., A.T., R.W.L., N.C.W., N.A.S., and P.N.S. contributed new reagents/analytic tools; W.C., S.-S.F., N.E.R., K.-C.S., L.J.H., B.L.H., and B.A.L. analyzed data; and W.C. and S.M. wrote the paper.

The authors declare no conflict of interest.

This article is a PNAS Direct Submission.

See Commentary on page 5767.

[1]Present address: Department of Genome Biology, The John Curtin School of Medical Research, The Australian National University, Canberra, ACT 0200, Australia.

[2]To whom correspondence should be addressed. E-mail: s.mahalingam@griffith.edu.au.

This article contains supporting information online at www.pnas.org/lookup/suppl/doi:10.1073/pnas.1318859111/-/DCSupplemental.

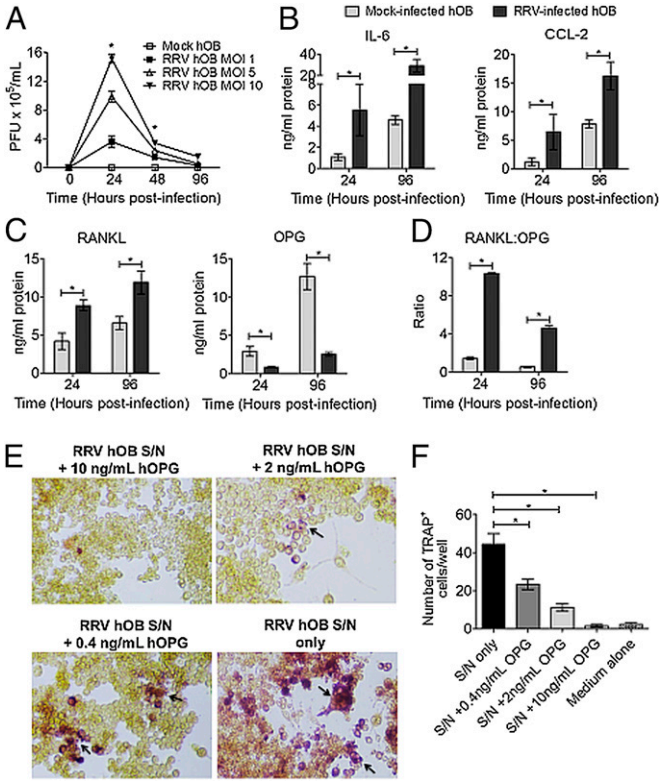

Fig. 1. RRV replicates in primary hOBs and disrupts the RANKL/OPG ratio. Primary hOBs were infected with RRV or treated with medium without virus (mock). (*A*) The amount of infectious virus in the supernatants was determined by plaque assay. Each data point represents the mean ± SEM of primary hOBs from seven healthy individuals, performed in duplicate. *$P <$ 0.001 using two-way ANOVA with Bonferroni posttest. (*B*) IL-6, CCL2, (*C*) RANKL and OPG protein levels in mock- and RRV-infected hOBs supernatants were determined by ELISA, and the (*D*) RANKL/OPG ratio is shown. Data shown are mean ± SEM, performed in duplicate. *$P < 0.05$, using Student *t* test, comparing mock- and RRV-infected. (*E*) Supernatants were tested for the ability to induce TRAP+ multinuclear cells from RAW264.7 cells, in the presence and absence of recombinant hOPG. RAW264.7 cells were cultured either with 10 ng/mL, 2 ng/mL, or 0.4 ng/mL hOPG, or with supernatants collected from RRV-infected hOBs at 96 h.p.i. Cells were stained for TRAP, with no counterstaining, after 8 d and visualized using light microscopy (20×). Arrows indicate TRAP+ cells. (*F*) The number of TRAP+ multinuclear cells (OC-like cells) per well was quantified. Images shown are representative of three independent experiments. Data are presented as mean ± SEM, performed in triplicate. *$P < 0.05$ using one-way ANOVA with Tukey's posttest. S/N, supernatant.

phenotypically characterized (Fig. S1) and infected with RRV–EGFP at a multiplicity of infection (MOI) of 1, 5, or 10. The virus titer increased for all MOIs, peaking at 24 h postinfection (h.p.i.) and declining to almost undetectable levels by 96 h.p.i. (Fig. 1*A*). These findings demonstrate that hOBs are susceptible to infection by RRV and suggest OB as a cellular target for arthritogenic alphaviruses.

Proinflammatory cytokines and chemokines are involved in the pathogenesis of alphaviral arthritides (6, 7). At 24 and 96 h.p.i., we performed ELISA and qualitative RT-PCR (qRT-PCR) analysis to evaluate cytokine/chemokine levels in mock- and RRV-infected hOBs. A correlation was observed between protein and mRNA expression (Fig. S2*A*), where IL-6 and CCL2 were significantly increased ($P < 0.05$) in RRV-infected hOBs compared with mock controls (Fig. 1*B*). Similarly, IL-1β levels increased significantly ($P < 0.05$) in response to RRV infection (Fig. S2 *B* and *C*). TNF-α mRNA expression was transient and declined to a level comparable to mock controls, although TNF-α protein was not detected (Fig. S2 *B* and *C*). These findings show that RRV infection of hOBs stimulated the production of proinflammatory factors IL-6, CCL2 and IL-1β, which are known to promote osteoclastogenesis (12, 20, 21).

To define the role of OBs in RRV infection, RANKL and OPG were measured in the supernatants of mock- and RRV-infected hOBs. At 24 and 96 h.p.i., RANKL levels were significantly ($P < 0.05$) increased in RRV-infected hOBs. In contrast, OPG was significantly ($P < 0.05$) lower in the RRV-infected cultures compared with mock controls (Fig. 1*C*). As a result, the RANKL/OPG ratio was markedly increased at 24 and 96 h.p.i. (Fig. 1*D*). Therefore, RRV infection disrupts the RANKL/OPG balance in hOBs, which suggests that RRV infection may affect osteoclastogenesis.

Primary hOBs Enhance Osteoclastogenesis in Response to RRV Infection. Osteoclastogenesis is regulated by OBs in the context of physiological bone remodelling, and disruption of the RANKL/OPG system can tilt the balance toward bone resorption (22). At 96 h.p.i., supernatants from RRV-infected hOBs were tested for their ability to induce Tartrate-resistant acid phosphatase (TRAP)-positive (TRAP+) multinuclear cells from mouse leukaemic monocyte macrophage cell line (RAW264.7 cells) as a model of osteoclastogenesis. As a positive control, RAW264.7 cells were differentiated to TRAP+ cells using recombinant human RANKL (hRANKL), in a process that could be inhibited using recombinant human OPG (hOPG) (Fig. S3*A*). The dose-dependent inhibition of hRANKL by hOPG is shown in Fig. S3*B*. RAW264.7 cells were cultured with supernatants from RRV-infected hOBs, and TRAP+ multinuclear cell formation was inhibited with the increasing levels of hOPG (Fig. 1*E*). The number of TRAP+ cells decreased ($P < 0.05$) with increasing levels of hOPG (Fig. 1*F*). RRV-infected RAW264.7 cells did not differentiate into TRAP+ cells, suggesting that RRV-infected RAW264.7 cells alone cannot induce osteoclastogenesis in the absence of OBs (Fig. S4*A*). Consistent with the results with hOBs, RAW264.7 cells cultured with 24 h supernatant from RRV-infected primary murine OBs (mOBs) showed a clear increase in TRAP+ cells after 6 d in culture, compared with those treated with supernatant from mock-infected OBs (Fig. S4*B*). Together, these data suggest that RRV infection of OBs can induce osteoclastogenesis in a RANKL-dependent manner.

RANKL/OPG Disruption in Synovial Fluid and Elevated Serum Levels of TRAP5B in RRV Patients. Pathologic bone loss in inflammatory arthritis is in part due to increased bone resorption, leading to an imbalance in the coordinated action of bone-forming OBs and bone-resorbing OCs (23, 24). In the synovial fluid of RRV patients, RANKL protein levels were higher, and OPG protein levels were lower than in healthy controls (Fig. 2*A*). This resulted in a markedly elevated RANKL/OPG ratio in RRV patients (Fig. 2*B*). In addition, serum TRAP5b levels were significantly ($P < 0.05$) higher in RRV patients (Fig. 2*C*), indicating increased osteoclastogenesis in response to RRV infection.

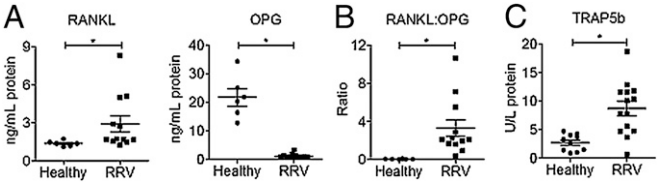

Fig. 2. RRV infection perturbs the RANKL/OPG ratio in RRV-infected patients. (*A*) Synovial fluid from healthy ($n = 6$) and RRV patients ($n = 12$) were tested for RANKL and OPG protein levels, and the (*B*) RANKL/OPG ratio is shown. (*C*) Serum from healthy ($n = 10$) and RRV patients ($n = 14$) was tested for TRAP5b. Data are presented as mean ± SEM. Each symbol represents an individual patient.*$P < 0.01$ using Mann–Whitney *U* test.

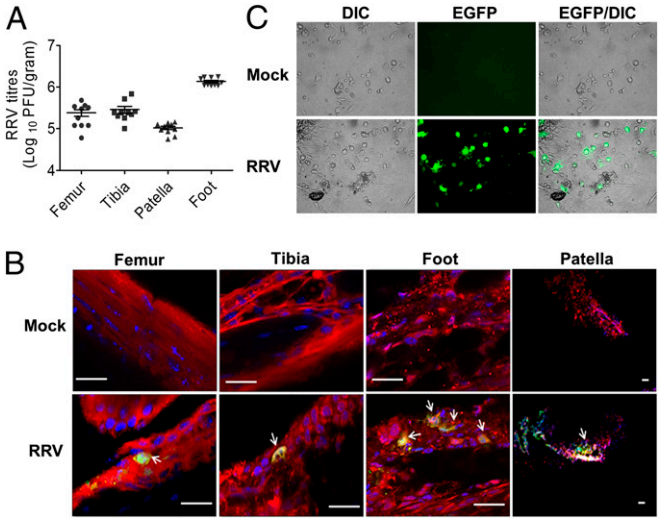

Fig. 3. RRV replicates in murine bones. Twenty-one–d-old C57BL/6 WT mice were infected s.c. with 10^6 pfu of RRV–EGFP or with diluent alone. (*A*) At day 2 p.i., the femur, tibia, patella, and foot from mock- and RRV-infected mice (n = 10) were collected and homogenized, and the presence of infectious virus determined by plaque assays. (*B*) Hind limbs of mock- and RRV-infected mice were removed, fixed in 4% PFA, decalcified in 14% EDTA, and cryosectioned (5 μm). Osteocalcin (red), replicating RRV–GFP (green, white arrows) and nuclei (blue), was visualized by confocal microscopy. (Scale bar, 30 μm.) (*C*) Osteoblastic cell fractions (F3 and F4) were isolated from knee joints of C57BL/6 WT mice and infected with RRV–EGFP at an MOI of 0.1 or with PBS (mock). At 24 h.p.i., mock- and RRV-infected bone tissues were visualized for EGFP by fluorescence microscopy (20×). F1, fraction 1; F2, fraction 2; F3, fraction 3; F4, fraction 4. DIC, differential interference contrast.

RRV Replicates in Murine Bone Cells and Induces Bone Loss. To determine if RRV can replicate in bone, RRV-infected WT mice were killed and the femur, tibia, patella, and foot collected for measurement of virus titers by plaque assay, with high viral titers detected in each of these sites (Fig. 3*A*). To further investigate if RRV localizes in bone tissue during infection, mock- and RRV-infected mice were killed and perfused with phosphate buffer saline (PBS), and their hind limbs were decalcified and cryosectioned. RRV replication, observed as EGFP expression, was detected in cells lining the periosteum of femur, tibia, and foot and in the patella (Fig. 3*B*). In a separate experiment, we demonstrated RRV replication in ex vivo OB-enriched cell preparations as determined by GFP expression (Fig. 3*C*). Although RRV replication was detected in joint cell fractions, the virus titers in fractions 3 and 4 (osteoblastic bone cells) were significantly higher ($P < 0.001$) than in fractions 1 and 2 (bone marrow cells, reticulocytes, and leukocytes) (Fig. S5*A*). Furthermore, fraction 3 and 4 cultures maintained detectable RRV replication until day 21 p.i., whereas RRV was only detectable in fractions 1 and 2 at day 1 p.i. (Table S1). In murine ex vivo OB cultures, the gene transcripts of IL-6, CCL2, IL-1β, and, to a lesser extent, TNF-α were clearly induced in response to RRV infection (Fig. S5*B*). These findings indicate that OBs are targets for RRV infection and are a source of proinflammatory factors during natural infection.

Using the established murine model of RRV infection, the impact of infection on bone architecture was evaluated by μCT. By day 15 p.i., μCT imaging showed clear bone loss in the tibial epiphysis, metatarsal joints, and vertebrae of RRV-infected mice, suggesting that RRV-induced bone loss is systemic (Fig. 4 *A* and *B*). In the tibial epiphysis and vertebrae of RRV-infected mice, bone volume was reduced by 10%, accompanied by a decrease in trabecular thickness (Tb.Th), as observed compared with saline-injected controls (Fig. 4 *C* and *D*). In addition, the width of growth plate and cortical bones of RRV-infected mice were significantly reduced compared with control mice (Fig. 5 *A* and *B*), indicating impairment in growth due to the infection. Histologic analysis also confirmed increased TRAP+ OCs (Fig. S6) and bone loss in the tibial epiphysis (Fig. 5*C*). These data are consistent with the disrupted RANKL/OPG ratio and high TRAP5b levels observed in RRV patients.

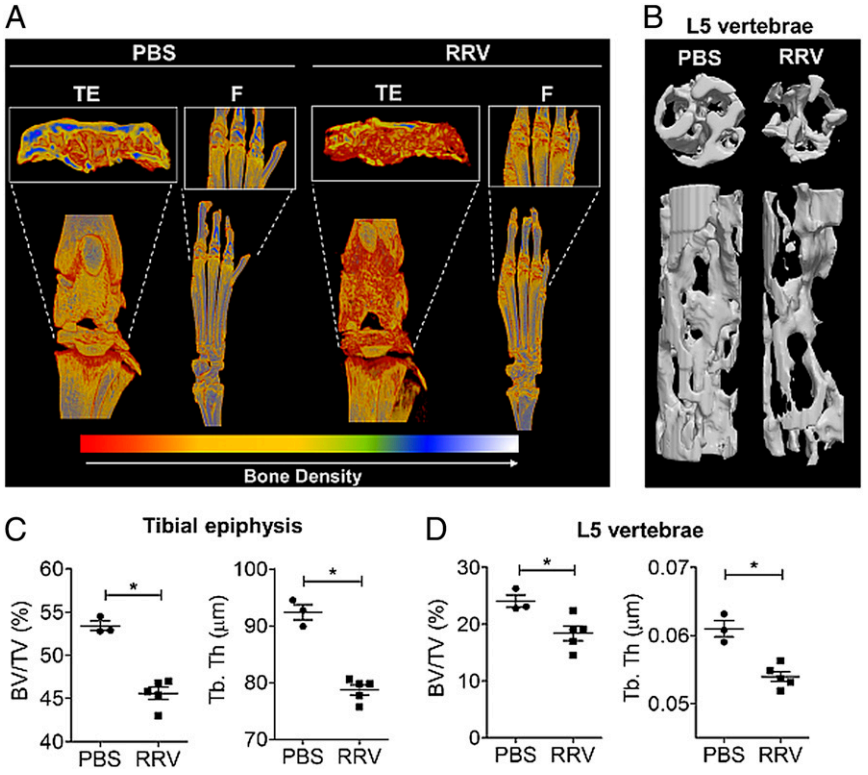

Fig. 4. Bone phenotype of RRV-infected C57BL/6 mice. μCT surface reconstruction performed in (*A*) hind limbs and (*B*) L5 vertebrae of mock- and RRV-infected WT mice (day 15 p.i.). BV/TV and Tb.Th in the (*C*) proximal tibial epiphysis and (*D*) L5 vertebrae of mock- and RRV-infected mice at day 15 p.i. are shown. *$P < 0.05$, using Student t test, comparing mock- and RRV-infected. Images of proximal tibial epiphysis, foot, and vertebrae represent observations in 3–5 mice per group. Each symbol represents a single mouse. Data represent mean ± SEM of 3–5 mice. F, foot; TE, tibial epiphysis.

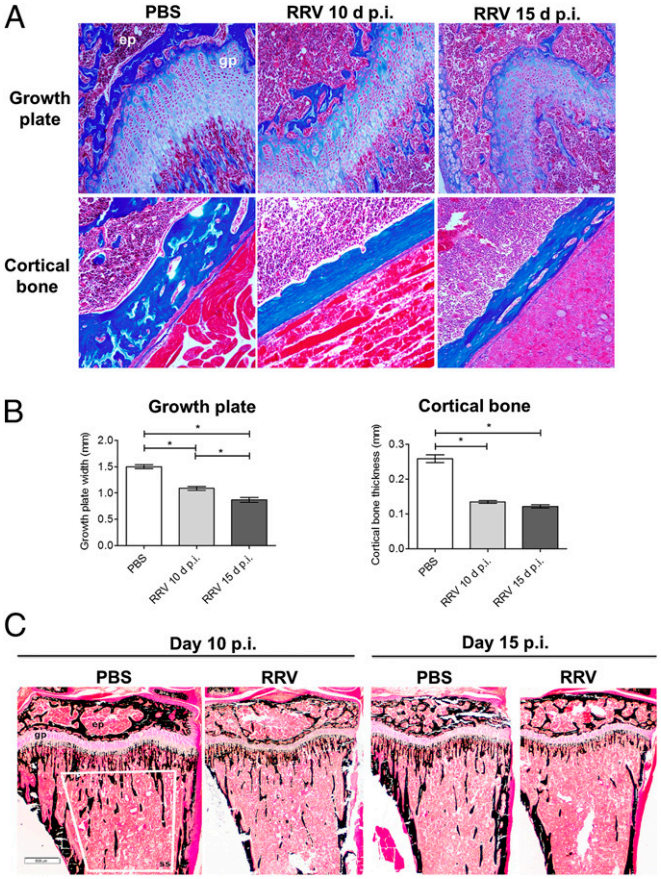

Fig. 5. RRV infection reduces growth plate width and cortical bone thickness. (*A*) Paraffin-sectioned (5 μm) sections from proximal tibia of mock- and RRV-infected WT mice were stained with Masson's trichrome stain at day 10 and 15 after infection (20×). Representative images from three to five mice per group are shown. (*B*) The width of cortical bones and growth plates of mock- and RRV-infected WT mice from five areas were measured. Data represent mean ± SEM of 3–5 mice per group. $*P < 0.05$ using one-way ANOVA with Turkey's posttest. (*C*) Plastic-embedded sections (5 μm) of tibiae from mock- and RRV-infected mice are stained with von Kossa stain at day 10 and 15 after infection (20×). C, cortical bone; GP, growth plate; M, muscles; TE, tibial epiphysis.

IL-6 Neutralization Prevented RRV-Induced Increases in the RANKL/OPG Ratio and Bone Loss. To investigate the role of IL-6 in RRV-induced bone loss, hind limbs from WT mice and mice treated with an IL-6 neutralizing antibody were collected at day 10 p.i. for μCT analysis. Reduced IL-6 protein levels in antibody-treated mice at day 10 p.i. were confirmed by ELISA (Fig. S7*A*). In response to RRV infection, WT mice showed severe bone loss at day 10 p.i. compared with control mice (Fig. 6*A*). However, IL-6 inhibition in RRV-infected mice ameliorated bone loss (Fig. 6*B*), preserving bone volume/tissue volume (BV/TV) and Tb.Th (Fig. 6C) compared with control RRV-infected mice. This implicates IL-6 as a key mediator of RRV-induced bone loss. The serum RANKL/OPG ratio in IL-6 neutralized mice was also significantly ($P < 0.001$) reduced compared with infected control mice, and did not differ from mock controls (Fig. 6*D*), suggesting that IL-6 plays a significant role in triggering alphavirus-induced bone loss in part by increasing the RANKL/OPG ratio. Although IL-6 neutralization significantly reduced RRV clinical score during early disease, it had no effect at peak RRVD (day 10 p.i.), nor did it improve weight gain in these animals (Fig. S7*B*). RRV titres in the ankle joints of IL-6 neutralized mice were significantly reduced compared with isotype control mice (Fig. S7*C*), suggesting that IL-6 also dampens viral clearance.

Discussion

Previous research on arthritogenic alphavirus-induced inflammation has revealed that the progression of musculoskeletal damage is mediated by proinflammatory cytokines and chemokines produced in response to infection (25–27). However, the exact mechanisms and inflammatory factors involved in alphavirus-induced arthralgia in bone tissues are not known. The synovial fluid of RRV-infected patients showed an imbalanced RANKL/OPG ratio, together with high serum TRAP5b levels, suggesting that RRV infection can result in increased osteoclastogenesis. Abnormally high bone resorption contributes to joint erosions and systemic bone loss, both hallmarks of RA. Similarly, radiographic evidence of bone erosions has been reported in CHIKV-infected patients (9, 28, 29). We demonstrate that RRV infection results in bone loss using an established murine model of RRV-induced arthritis. The proximal tibial epiphysis, dorsal metatarsophalangeal joints of the foot, and vertebrae of infected mice showed reduced bone volume, suggesting that increased osteoclastogenesis in response to RRV infection can induce bone loss. The murine model of RRV infection showed severe disease signs characterized by reduced growth plate width, hind-limb weakness, and dragging (25). Replication of Sindbis-group alphaviruses has been described in murine long bones (30), and here we demonstrate previously unidentified high levels of infectious RRV in bones, specifically the femur, tibia, foot, and patella. Cells lining the periosteum in multiple bones of hind limbs were infected by RRV. In addition, RRV infects murine ex vivo OB cells effectively during the early phase of infection and support persistent infections up to day 21 p.i. Therefore, these findings suggest that RRV-infected osteoblastic cells may contribute to the pathogenesis of RRV-induced polyarthritis.

OBs play an important role in regulating osteoclastogenesis through their regulated expression of RANKL and OPG, with an increased RANKL/OPG ratio creating proosteoclastic conditions within the local bone microenvironment (22, 24). Non-osteoblastic cells with elevated RANKL expression, such as T cells and synovial fibroblasts, also contribute to regulating OC differentiation and bone loss in inflammatory arthritis (20, 31). In response to RRV infection, hOBs showed an increase in RANKL expression, whereas OPG expression decreased. Hence, our findings highlight the potential role of OBs in RRV pathogenesis and provide previously unidentified evidence of OB involvement in alphaviral-induced disease. OBs interact with precursor monocytic cells through RANKL/RANK to induce maturation of OCs in vivo (32). This system can be modeled in vitro using RAW264.7 cells, which have the capacity to differentiate into TRAP+ multinuclear OCs in the presence of hRANKL (33). RRV-infected hOBs enhanced osteoclastogenesis through disruption of the RANKL/OPG ratio. This result is consistent with an increase in circulating serum TRAP5b in RRV patients. Recently, alterations in the RANKL/OPG ratio have been reported in CHIKV-infected hOBs (11), suggesting that our findings may be broadly applicable to other arthritogenic viruses. Therefore, the elevation in RANKL and suppression of OPG expression highlight the likelihood that OBs may play an important role in the development of persistent musculoskeletal symptoms in arthritogenic alphavirus-induced disease.

Our work also demonstrates that IL-6 is a critical mediator of the RRV-induced increase in RANKL/OPG ratio and bone loss. Several inflammatory cytokines and chemokines play key roles in both the regulation of factors that influence bone remodelling and the pathogenesis of alphavirus infection (34). In alphavirus-induced arthralgia, IL-6 is expressed in affected joints (35) and a role for IL-6 in determining alphavirus disease severity has been proposed (7, 26). Skeletal muscles (36) and cells of bones (37) can produce IL-6, which is highly elevated and associated with persistent arthralgia in chronic alphaviral infections (7, 38). IL-6 is a pleiotropic cytokine important in regulating immune responses and bone metabolism in diseases such as osteoporosis and Paget disease (39, 40), and mediates increased osteoclastogenesis in murine models of ovariectomy-induced (41) and

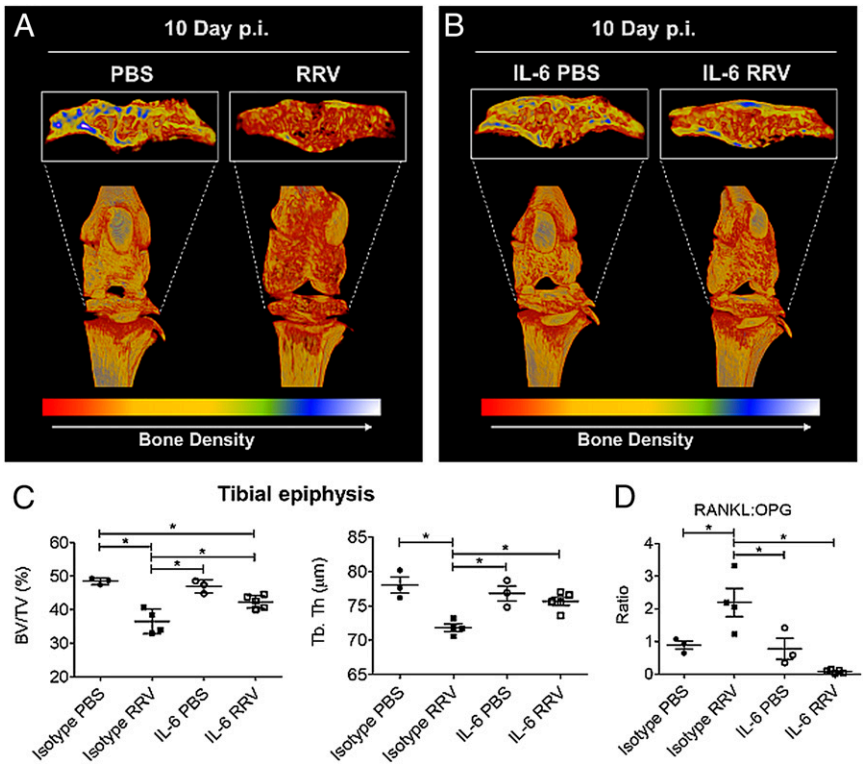

Fig. 6. Treatment with IL-6 neutralizing antibody ameliorates RRV-induced bone loss in C57BL/6 mice. μCT surface reconstruction performed in hind limbs from RRV-infected (*A*) WT and (*B*) IL-6 neutralized mice at day 10 after infection. Images of proximal tibial epiphysis represent observations in 3–5 mice per group. (*C*) BV/TV, Tb.Th in the proximal tibial epiphysis, and (*D*) RANKL/OPG ratio in the serum from mock- or RRV-infected and Rat IgG1 isotype control or IL-6 neutralizing antibody treated mice at day 10 p.i. are shown. $*P < 0.05$ using one-way ANOVA with Turkey's posttest. Each symbol represents a single mouse. Data represent mean ± SEM of 3–5 mice per group.

arthritic (42) bone loss. In addition, IL-6 has a central role in the up-regulation of RANKL in OBs (10, 11), the induction of CCL2 (43), and the development of joint pain (44). In fact, low bone mass and high OC numbers have been reported in the growing skeleton of transgenic IL-6 mice, a model of chronic inflammation (45). We have shown that RRV-induced bone loss is ameliorated in the absence of IL-6, suggesting that IL-6 is a crucial osteotropic factor that regulates bone loss during RRVD.

Our work provides unique insights into the bone pathophysiology in alphavirus-induced arthralgia. The alteration in the RANKL/OPG ratio toward bone resorption contributes to increasing osteoclastogenesis and possibly the aggravation of arthralgia after RRV infection. Our study highlights a possible OB-mediated mechanism that contributes to inflammation-induced bone loss following RRV infection through RANKL-mediated osteoclastogenesis. We showed that IL-6 is essential for bone loss during RRV infection and inhibition of IL-6 alleviates inflammation during early RRVD but not in later stages of the disease, suggesting that RRV-induced bone loss may be driven by early inflammatory responses. Therefore, targeting IL-6 in early RRVD using anti–IL-6R antibodies, such as tocilizumab, will likely be therapeutically beneficial in the prevention of RRV-induced bone loss.

Materials and Methods

Viruses. Stocks of T48 strain of RRV (RRV-T48) were generated from the full-length T48 cDNA clone (46). Stocks of RRV that expressed EGFP were kindly provided by Mark Heise (University of North Carolina at Chapel Hill, Chapel Hill, NC). RRV titres were determined by plaque assay on Vero cells as described previously (47).

Mice. C57BL/6 WT mice were obtained from the Animal Resource Centre and bred in-house. The 21-d-old male and female mice, of equal distribution, were inoculated s.c. in the thorax below the right forelimb with 10^4 pfu of RRV-T48 or 10^6 pfu of RRV–EGFP diluted in PBS as described (47). Mice were monitored daily for diet and well-being. Mice were weighted and scored for disease signs every 24 h as described previously (27). All animal experiments were approved by the Animal Ethics Committee of Griffith University (BDD/06/11/AEC).

IL-6 Neutralization in Vivo. Twenty-one-d-old WT mice received injections of neutralizing anti–IL-6 antibody (MP5-20F3, BioXcell) or Rat IgG1 isotype control: 500 μg intraperitoneally at day 0 and at days 2, 4, 6, and 8 p.i. Mice were killed and serum collected at day 10 postinfection. Hind limbs were fixed in 4% (wt/vol) paraformaldehyde (PFA) and stored in 70% ethanol.

Histology. Mice were killed, hind limbs collected, fixed in 4% (wt/vol) PFA, decalcified, and embedded in paraffin or plastic. Five micrometer sections were prepared and stained with TRAP, Masson's trichrome, and von Kossa stains.

Primary Cell Cultures. Primary mOBs were obtained from the calvarial bones of C57BL/6 WT mice, of equal sex distribution, as described previously with minor modifications (48). Murine joint cell fractions were generated according to the amount of time exposed to collagenase digestion as described previously (30, 49). Primary hOBs were obtained from trabecular bone specimens of seven healthy individuals (four males, three females) aged 50–60 y undergoing orthopedic operations for causes unrelated to arthritis or osteoporosis. The hOBs were cultured from bone fragments as described previously (50). See *SI Materials and Methods* for details.

Patient Samples. Convalescent serum samples from 14 RRV patients (age range, 21–66 y; male to female ratio, 7:7) serologically confirmed with IgG anti-RRV were provided by Andrew Lloyd (University of New South Wales, Kensington, Australia). Serum samples from 13 healthy individuals (age range, 18–65 y; male to female ratio, 7:6) were provided by the Australian Red Cross. Twelve synovial fluid samples from patients with RRV-induced polyarthritis (age range, 30–45 y; male to female ratio, 6:6) were provided by The Royal Melbourne Hospital. Synovial fluids from six healthy individuals (age range, 47–60 y; male to female ratio, 3:3) for causes unrelated to arthritis or osteoporosis were provided by Australian National University Medical School. All human samples were collected with informed consent and human ethics approval.

OC-Like Cell Differentiation Assays. RAW264.7 cells were cultured with supernatant from RRV-infected hOBs. After 8 d in culture, cells were fixed for detection of TRAP enzyme activity. See *SI Materials and Methods* for details.

TRAP Histochemical Staining. Cells were fixed in 4% (wt/vol) PFA, and TRAP enzyme activity was detected using Sigma-Aldrich kit 387-A according to the manufacturer's instructions. For in vitro inhibition of TRAP+ cell differentiation, see *SI Materials and Methods* for details.

μCT. μCT analyses were performed on murine hind limbs with Skyscan 1076 μ-CT system (Skyscan). BV/TV and Tb.Th were determined using CTAN (Skyscan). See *SI Materials and Methods* for details.

ELISAs. See *SI Materials and Methods* for details.

Plaque Assays. See *SI Materials and Methods* for details.

qRT-PCR. See *SI Materials and Methods* for details.

Immunofluorescence. See *SI Materials and Methods* for details.

Statistical Analysis. Viral titers, RT-PCR, ELISA, clinical scores, and bone density analysis were statistically evaluated by two-tailed unpaired Student *t* tests or one-way ANOVA with Tukey's posttest. Plaque assays for primary hOBs, weight gain, and clinical scores were analyzed by two-way ANOVA with Bonferroni posttest. TRAP+ cell quantification, cortical bone, and growth plate thickness were analyzed by one-way ANOVA with Tukey's posttest. All data were assessed for Gaussian distribution using the D'Agostino–Pearson normality test before analysis with these parametric tests. Statistics were performed with GraphPad Prism 5.02.

ACKNOWLEDGMENTS. The authors gratefully acknowledge the critical reading and expert advice provided by Drs. Mark Forwood (Griffith University, Australia), Andreas Suhrbier [Queensland Institute of Medical Research Berghofer (QIMR Berghofer), Australia], and Michael Rolph (Griffith University, Australia); we also acknowledge Dr. Mark Heise (University of North Carolina at Chapel Hill) for the assistance with murine ex vivo fractionation technique and Mr. Glynn Rees and QIMR Histochemistry Laboratory for immunohistochemical staining. S.M. is the recipient of the Australian Research Council Future Fellowship. This project was supported by funding from the Australian National Health and Medical Research Council Grants508600 and APP1012292 (to S.M.).

1. Foo SS, et al. (2011) The genetics of alphaviruses. *Future Virology* 6(12):1407–1422.
2. Kelly-Hope LA, Kay BH, Purdie DM, Williams GM (2002) The risk of Ross River and Barmah Forest virus disease in Queensland: implications for New Zealand. *Aust N Z J Public Health* 26(1):69–77.
3. Klapsing P, et al. (2005) Ross River virus disease reemergence, Fiji, 2003-2004. *Emerg Infect Dis* 11(4):613–615.
4. Harley D, Bossingham D, Purdie DM, Pandeya N, Sleigh AC (2002) Ross River virus disease in tropical Queensland: Evolution of rheumatic manifestations in an inception cohort followed for six months. *Med J Aust* 177(7):352–355.
5. Rulli NE, Melton J, Wilmes A, Ewart G, Mahalingam S (2007) The molecular and cellular aspects of arthritis due to alphavirus infections: Lesson learned from Ross River virus. *Ann N Y Acad Sci* 1102:96–108.
6. Chaaitanya IK, et al. (2011) Role of proinflammatory cytokines and chemokines in chronic arthropathy in CHIKV infection. *Viral Immunol* 24(4):265–271.
7. Chow A, et al. (2011) Persistent arthralgia induced by Chikungunya virus infection is associated with interleukin-6 and granulocyte macrophage colony-stimulating factor. *J Infect Dis* 203(2):149–157.
8. Russell RC (2002) Ross River virus: Ecology and distribution. *Annu Rev Entomol* 47(1):1–31.
9. Manimunda SP, et al. (2010) Clinical progression of chikungunya fever during acute and chronic arthritic stages and the changes in joint morphology as revealed by imaging. *Trans R Soc Trop Med Hyg* 104(6):392–399.
10. Her Z, et al. (2012) Reply to Noret et al. *J Infect Dis* 206(3):457–459.
11. Noret M, et al. (2012) Interleukin 6, RANKL, and osteoprotegerin expression by chikungunya virus-infected human osteoblasts. *J Infect Dis* 206(3):455–457, 457–459.
12. Liu XH, Kirschenbaum A, Yao S, Levine AC (2005) Cross-talk between the interleukin-6 and prostaglandin E(2) signaling systems results in enhancement of osteoclastogenesis through effects on the osteoprotegerin/receptor activator of nuclear factor-kappaB (RANK) ligand/RANK system. *Endocrinology* 146(4):1991–1998.
13. Mori T, et al. (2011) IL-1β and TNFα-initiated IL-6-STAT3 pathway is critical in mediating inflammatory cytokines and RANKL expression in inflammatory arthritis. *Int Immunol* 23(11):701–712.
14. Mateo L, et al. (2000) An arthrogenic alphavirus induces monocyte chemoattractant protein-1 and interleukin-8. *Intervirology* 43(1):55–60.
15. Pavkova Goldbergova M, et al. (2012) RANTES, MCP-1 chemokines and factors describing rheumatoid arthritis. *Mol Immunol* 52(3-4):273–278.
16. Goldring SR (2003) Pathogenesis of bone and cartilage destruction in rheumatoid arthritis. *Rheumatology (Oxford)* 42(Suppl 2):ii11–ii16.
17. Nakamura I, Takahashi N, Jimi E, Udagawa N, Suda T (2012) Regulation of osteoclast function. *Mod Rheumatol* 22(2):167–177.
18. Ainola M, Mandelin J, Liljeström M, Konttinen YT, Salo J (2008) Imbalanced expression of RANKL and osteoprotegerin mRNA in pannus tissue of rheumatoid arthritis. *Clin Exp Rheumatol* 26(2):240–246.
19. van Tuyl LHD, et al. (2010) Baseline RANKL:OPG ratio and markers of bone and cartilage degradation predict annual radiological progression over 11 years in rheumatoid arthritis. *Ann Rheum Dis* 69(9):1623–1628.
20. Souza PP, Lerner UH (2013) The role of cytokines in inflammatory bone loss. *Immunol Invest* 42(7):555–622.
21. Binder NB, et al. (2009) Estrogen-dependent and C-C chemokine receptor-2-dependent pathways determine osteoclast behavior in osteoporosis. *Nat Med* 15(4):417–424.
22. Boyce BF, Xing L (2008) Functions of RANKL/RANK/OPG in bone modeling and remodeling. *Arch Biochem Biophys* 473(2):139–146.
23. Firestein GS (2003) Evolving concepts of rheumatoid arthritis. *Nature* 423(6937):356–361.
24. Walsh NC, Gravallese EM (2010) Bone remodeling in rheumatic disease: A question of balance. *Immunol Rev* 233(1):301–312.
25. Lidbury BA, Simeonovic C, Maxwell GE, Marshall ID, Hapel AJ (2000) Macrophage-induced muscle pathology results in morbidity and mortality for Ross River virus-infected mice. *J Infect Dis* 181(1):27–34.
26. Lidbury BA, et al. (2008) Macrophage-derived proinflammatory factors contribute to the development of arthritis and myositis after infection with an arthrogenic alphavirus. *J Infect Dis* 197(11):1585–1593.
27. Herrero LJ, et al. (2011) Critical role for macrophage migration inhibitory factor (MIF) in Ross River virus-induced arthritis and myositis. *Proc Natl Acad Sci USA* 108(29):12048–12053.
28. Bouquillard É, Combe B (2009) A report of 21 cases of rheumatoid arthritis following Chikungunya fever. A mean follow-up of two years. *Joint Bone Spine* 76(6):654–657.
29. Malvy D, et al. (2009) Destructive arthritis in a patient with chikungunya virus infection with persistent specific IgM antibodies. *BMC Infect Dis* 9:200.
30. Heise MT, Simpson DA, Johnston RE (2000) Sindbis-group alphavirus replication in periosteum and endosteum of long bones in adult mice. *J Virol* 74(19):9294–9299.
31. Horwood NJ, et al. (1999) Activated T lymphocytes support osteoclast formation in vitro. *Biochem Biophys Res Commun* 265(1):144–150.
32. Yasuda H, et al. (1998) Osteoclast differentiation factor is a ligand for osteoprotegerin/osteoclastogenesis-inhibitory factor and is identical to TRANCE/RANKL. *Proc Natl Acad Sci USA* 95(7):3597–3602.
33. Kwan Tat S, et al. (2008) The differential expression of osteoprotegerin (OPG) and receptor activator of nuclear factor kappaB ligand (RANKL) in human osteoarthritic subchondral bone osteoblasts is an indicator of the metabolic state of these disease cells. *Clin Exp Rheumatol* 26(2):295–304.
34. Kwan Tat S, Padrines M, Théoleyre S, Heymann D, Fortun Y (2004) IL-6, RANKL, TNF-alpha/IL-1: Interrelations in bone resorption pathophysiology. *Cytokine Growth Factor Rev* 15(1):49–60.
35. Hoarau J-J, et al. (2010) Persistent chronic inflammation and infection by Chikungunya arthritogenic alphavirus in spite of a robust host immune response. *J Immunol* 184(10):5914–5927.
36. Febbraio MA, Pedersen BK (2002) Muscle-derived interleukin-6: Mechanisms for activation and possible biological roles. *FASEB J* 16(11):1335–1347.
37. Sims NA, Walsh NC (2010) GP130 cytokines and bone remodelling in health and disease. *BMB Rep* 43(8):513–523.
38. Lohachanakul J, Phuklia W, Thannagith M, Thonsakulprasert T, Ubol S (2012) High concentrations of circulating interleukin-6 and monocyte chemotactic protein-1 with low concentrations of interleukin-8 were associated with severe chikungunya fever during the 2009-2010 outbreak in Thailand. *Microbiol Immunol* 56(2):134–138.
39. Roodman GD, et al. (1992) Interleukin 6. A potential autocrine/paracrine factor in Paget's disease of bone. *J Clin Invest* 89(1):46–52.
40. Tsangari H, Findlay DM, Kuliwaba JS, Atkins GJ, Fazzalari NL (2004) Increased expression of IL-6 and RANK mRNA in human trabecular bone from fragility fracture of the femoral neck. *Bone* 35(1):334–342.
41. Poli V, et al. (1994) Interleukin-6 deficient mice are protected from bone loss caused by estrogen depletion. *EMBO J* 13(5):1189–1196.
42. Wong PK, et al. (2006) Interleukin-6 modulates production of T lymphocyte-derived cytokines in antigen-induced arthritis and drives inflammation-induced osteoclastogenesis. *Arthritis Rheum* 54(1):158–168.
43. Romano M, et al. (1997) Role of IL-6 and its soluble receptor in induction of chemokines and leukocyte recruitment. *Immunity* 6(3):315–325.
44. von Banchet GS, Kiehl M, Schaible H-G (2005) Acute and long-term effects of IL-6 on cultured dorsal root ganglion neurones from adult rat. *J Neurochem* 94(1):238–248.
45. De Benedetti F, et al. (2006) Impaired skeletal development in interleukin-6-transgenic mice: A model for the impact of chronic inflammation on the growing skeletal system. *Arthritis Rheum* 54(11):3551–3563.
46. Kuhn RJ, Niesters HG, Hong Z, Strauss JH (1991) Infectious RNA transcripts from Ross River virus cDNA clones and the construction and characterization of defined chimeras with Sindbis virus. *Virology* 182(2):430–441.
47. Morrison TE, et al. (2006) Characterization of Ross River virus tropism and virus-induced inflammation in a mouse model of viral arthritis and myositis. *J Virol* 80(2):737–749.
48. Bakker A, Klein-Nulend J (2003) Osteoblast isolation from murine calvariae and long bones. *Methods Mol Med* 80:19–28.
49. Gu G, Nars M, Hentunen TA, Metsikkö K, Väänänen HK (2006) Isolated primary osteocytes express functional gap junctions in vitro. *Cell Tissue Res* 323(2):263–271.
50. Smith PN, et al. (2010) Heparanase in primary human osteoblasts. *J Orthop Res* 28(10):1315–1322.